

## Preparation, Photoisomerization, and Microfabrication with Two-Photon Polymerization of Crosslinked Azo-Polymers

Hui Wang,<sup>1,2</sup> Feng Jin,<sup>1</sup> Shu Chen,<sup>1,2</sup> Xian-Zi Dong,<sup>1</sup> Yong-Liang Zhang,<sup>1</sup> Wei-Qiang Chen,<sup>1</sup> Zhen-Sheng Zhao,<sup>1</sup> Xuan-Ming Duan<sup>1</sup>

<sup>1</sup>Laboratory of Organic NanoPhotonics and Key Laboratory of Functional Crystals and Laser Technology, Technical Institute of Physics and Chemistry, Chinese Academy of Sciences, No. 29, Zhongguancun East Road, Beijing 100190, People's Republic of China

<sup>2</sup>Graduate University of Chinese Academy of Sciences, Beijing 100190, People's Republic of China

Correspondence to: X.-M. Duan (E-mail: xmduan@mail.ipc.ac.cn)

**ABSTRACT:** We report the preparation, photoisomerization properties, and three-dimensional (3D) microstructure fabrication with two-photon polymerization of crosslinked azo-polymers. A series of bi-acrylate-substituted azobenzene derivatives were designed and synthesized as the monomers and/or crosslinkers of the crosslinked azo-polymers. The doping concentration of the derivatives in prepolymer resins was significantly increased due to the introduction of bulky *tert*-butyl and flexible alkyl chains. The double-exponential dynamics of *trans*-to-*cis* photoisomerization of the azo-polymers indicated the coexistence of different processes for the azobenzene moieties in the polymeric crosslinked networks. The crosslinked azo-polymers exhibited ideal “on–off” switching performance in the highly reversible *trans*–*cis*–*trans* isomerization cycles. Furthermore, we prepared a photoresist containing the azobenzene derivative for 3D microstructure fabrication based on two-photon polymerization. A woodpile photonic crystal with a photonic bandgap at telecommunication wavelength region was successfully fabricated with the azobenzene-containing photoresist, which would open the way for the design and manufacturing of miniature optical communication devices. © 2013 Wiley Periodicals, Inc. *J. Appl. Polym. Sci.* 130: 2947–2956, 2013

**KEYWORDS:** synthesis and processing; photopolymerization; photochemistry; optical properties; crosslinking

Received 28 February 2013; accepted 5 May 2013; Published online 13 June 2013

DOI: 10.1002/app.39507

### INTRODUCTION

Azo-polymers have been intensively investigated since they are considered as potentially functional materials for the applications such as optical driven machine,<sup>1</sup> optical modulation,<sup>2</sup> optical storage,<sup>3–5</sup> polarization holography<sup>6,7</sup>, due to their well-known isomerization effect between their *trans* and *cis* forms by irradiation of ultraviolet light and reverse process taking place photochemically and/or thermally. Azo-polymers for nonlinear optical application have been mainly focused on the polymers containing azobenzene moieties as dye-doping and side-chain systems.<sup>8–10</sup> Crosslinked azo-polymers as well as photoisomerization effects have still merely investigated.

Crosslinked polymers have been widely used in photolithography as photoresist. In the past decade, two-photon polymerization (TPP) has been developed as an emerging stereolithography technique for fabricating complicated three-dimensional (3D) microstructures<sup>11</sup> under nanometer scaled resolution.<sup>12–14</sup>

Various functional materials including hybrid materials,<sup>15</sup> nanocomposites,<sup>16,17</sup> and metals<sup>18–20</sup> have been used for fabricating functional microstructures and microdevices with the multi-photon lithography technique. The functional devices including photonic crystals (PhCs),<sup>21,22</sup> optical waveguides,<sup>23,24</sup> microlens arrays,<sup>25,26</sup> and microemitters<sup>27</sup> fabricated by TPP exhibited potential possibilities in photonic applications. In our previous study, we proposed and demonstrated the preparation of an optical-driven PhC by using the photoresist contained an azobenzene derivative with acrylamide and 3-(acryloxy)propoxy moieties as monomers and crosslinkers.<sup>28</sup> The PhC composed of azo-polymers with azobenzene chromophores connected to the crosslinked polymeric backbones exhibited good photonic bandgap (PBG) tuning properties. However, the azobenzene derivatives tend to precipitate due to the aggregation induced by the hydrogen bonding interaction between the acrylamide groups,<sup>29</sup> which cause the photoresist to become opaque and degrade the ability of fabrication in TPP. Therefore, it is essential

Additional Supporting Information may be found in the online version of this article.

© 2013 Wiley Periodicals, Inc.

to design well-soluted azobenzene derivatives for improving the properties of photoresist during TPP fabrication process.

In this article, we report the preparation, photoisomerization properties, and 3D microstructure fabrication with TPP of crosslinked azo-polymers. A series of new azobenzene derivatives are designed, synthesized, and employed to prepare azo-polymers. Bulky *tert*-butyl group and flexible alkyl chains are introduced into the azobenzene chromophores to improve the doping concentration in pre-polymer resins and the photoresist. We investigate the laser-induced *trans*-to-*cis* photoisomerization behavior of azo-polymers by monitoring the ultraviolet–visible (UV–Vis) absorption spectra and demonstrate the relationship between dynamics and molecular structures. Furthermore, the woodpile PhCs with PBG in telecommunication wavelength region is successfully achieved by TPP with the photoresist containing the synthesized azobenzene derivative. Consequently, this study not only provides a method to obtain crosslinked azo-polymers with high concentration of azobenzene moieties but also exhibits the potential possibility for developing micro/nano-scale optical communication devices with optical functional azo-polymers.

## EXPERIMENTAL

### Materials

Triethylamine, acryloyl chloride, sodium nitrite, sodium hydroxide, phosphoric acid, hydrochloric acid, anhydrous potassium carbonate, anhydrous magnesium sulfate, 2,2′-azobisisobutyronitrile (AIBN), and all solvents were purchased from Beijing Chemical Reagent Company. 4-Aminophenol and methyl methacrylate (MMA) were provided by Tianjin Jinke Refined Chemical Engineering Institute. 2-*tert*-butylphenol was supplied by Alfa Aesar Co., Tianjin, China. 3-Chloropropan-1-ol and 6-chlorohexan-1-ol were purchased from J&K Chemicals. Photoinitiator benzil and photosensitizer 2-benzyl-2-(dimethylamino)-4′-morpholinobutyrophenone were commercially available from Acros Organics and Aldrich, respectively. Dipentaerythritol hexa-acrylate (trade name: Light Acrylate DPE-6A) was obtained from Kyoisha Chemical Co., Japan. AIBN was recrystallized from methanol. Dichloromethane and triethylamine were dried over calcium hydride and freshly distilled before use. Other reagents and solvents were of analytical grade and used as received without further purification.

### Characterization of Azobenzene Derivatives and Azo-Polymers

<sup>1</sup>H NMR spectra were recorded on an Avance II-400 spectrometer (Bruker, Germany) using CDCl<sub>3</sub> as a solvent and all shifts are referenced to tetramethylsilane (TMS). High resolution mass spectra (HRMS) were performed on Microflex (Bruker, Germany). Melting points were identified on an X-4 microscopic melting-point apparatus (Beijing Focus Instrument Company, China). Fourier transform infrared (FT-IR) spectra of azobenzene derivatives and azo-polymers were scanned over the range of 400–4000 cm<sup>-1</sup> with potassium bromide slice on an Excalibur 3100 spectrometer (Varian). Thermogravimetric analysis (TGA) was carried out with a Q-5000 derivatograph analyzer (TA Instruments) under a N<sub>2</sub> atmosphere at a scanning rate of 10°C/min. UV–Vis absorption spectra of azo-polymer films

were characterized by a UV-2550 spectrophotometer (Shimadzu, Japan). The refractive index of the azo-polymer film was measured with a Model 2010 prism coupler (Mettricon) instrument at the wavelength of 1315 nm.

### Synthesis of Azobenzene Derivatives

Azobenzene derivatives were synthesized according to previous procedures,<sup>30,31</sup> as shown in Scheme 1.

### Synthesis of 3-(*tert*-Butyl)-4,4′-dihydroxy-azobenzene (Azo-OH)

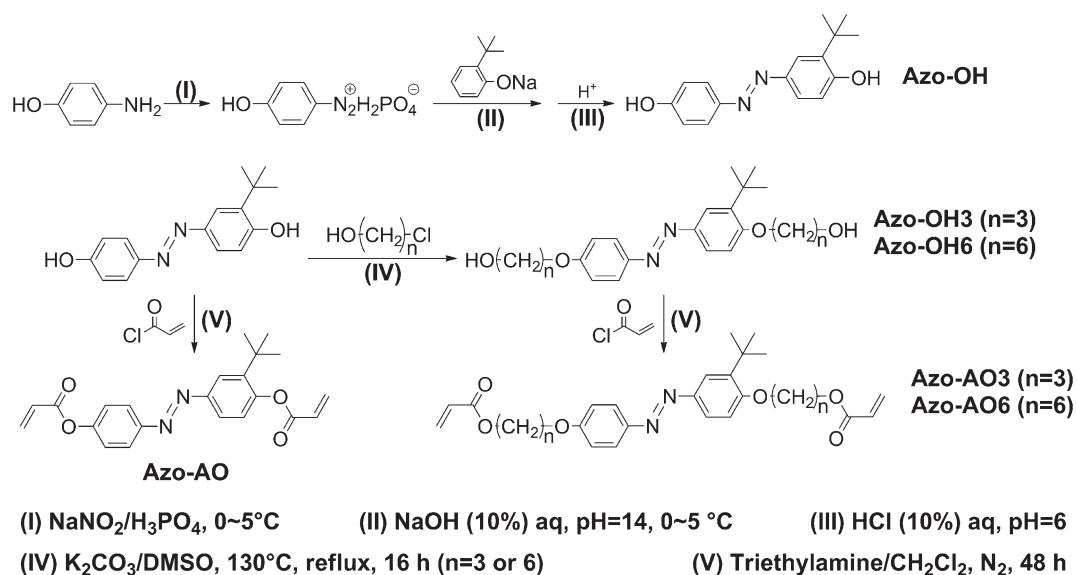
4-Aminophenol (3.27 g, 30 mmol) was suspended in 15 mL of H<sub>3</sub>PO<sub>4</sub>/water solution (volume ratio 1 : 1). The reaction system was submerged in an ice-water bath and the reaction temperature was strictly controlled between 2–5°C. NaNO<sub>2</sub> (2.07 g, 30 mmol) was dissolved in 3 mL of cooled deionized water and subsequently added dropwise into the reaction system with stirring. The mixture was kept stirring for 30 min further. A solution of sodium 2-*tert*-butylphenolate (4.50 g, 30 mmol) in 15 mL of water was then added immediately. Diazo-coupling reaction occurred when the pH of the mixture was adjusted to 12 with 10 wt % NaOH aqueous solution. The pH of the mixture was then adjusted to 6 with 10 wt % dilute hydrochloric acid and dark red solid precipitated from the reaction system. After filtration, washing with deionized water and drying in vacuum at 40°C, the crude product was purified by column chromatography using ethyl acetate–petroleum ether (1:3 v/v) as eluent to give brown solid. Yield = 33%; m.p. 192–194°C; <sup>1</sup>H NMR (400 MHz, CDCl<sub>3</sub>, δ ppm): 7.90 (d, 1H, *J* = 2.28 Hz), 7.83 (d, 2H, *J* = 8.84 Hz), 7.65 (dd, 1H, *J*<sub>1</sub> = 2.32 Hz, *J*<sub>2</sub> = 8.40 Hz), 6.93 (d, 2H, *J* = 8.84 Hz), 6.76 (d, 1H, *J* = 8.44 Hz), 5.09 (s, 1H), 4.97 (s, 1H), 1.47 (s, 9H); FT-IR (KBr, cm<sup>-1</sup>): 3398, 3168, 2960, 1590, 1509, 1432, 1389, 1282, 1216, 839; HRMS (C<sub>16</sub>H<sub>18</sub>N<sub>2</sub>O<sub>2</sub>): Calcd.: 270.1368; Obsd.: 270.1367 (–0.4 ppm).

### Synthesis of 3-(*tert*-Butyl)-4,4′-bis(3-hydroxypropoxy)-azobenzene (Azo-OH3)

To a 250 mL three-necked flask, Azo-OH (2.70 g, 10 mmol), K<sub>2</sub>CO<sub>3</sub> (5.52 g, 40 mmol), 3-chloropropan-1-ol (3.78 g, 40 mmol), and 100 mL of DMSO were added and the reaction system was heated from ambient temperature to 130°C and kept under refluxing state for 16 h. After cooling, the system was poured into 10 wt % NaOH aqueous solution and dark brown solid was precipitated. The insoluble was filtered, washed with deionized water, and purified by column chromatography using ethyl acetate–petroleum ether (1 : 1 v/v) as eluent to give a yellow solid. Yield = 84%; m.p. 129–130°C; <sup>1</sup>H NMR (400 MHz, CDCl<sub>3</sub>, δ ppm): 7.91 (d, 1H, *J* = 2.40 Hz), 7.87 (d, 2H, *J* = 8.92 Hz), 7.74 (dd, 1H, *J*<sub>1</sub> = 2.40 Hz, *J*<sub>2</sub> = 8.68 Hz), 7.01 (d, 2H, *J* = 8.96 Hz), 6.99 (d, 1H, *J* = 8.68 Hz), 4.22 (m, 2H), 4.21 (m, 2H), 3.95 (m, 2H), 3.90 (m, 2H), 2.16 (m, 2H), 2.09 (m, 2H), 1.68 (s, 1H), 1.46 (s, 9H); FT-IR (KBr, cm<sup>-1</sup>): 3382, 2955, 2871, 1600, 1499, 1466 1416, 1393, 1314, 1236, 1172, 1143, 1080, 1058, 841; HRMS (C<sub>22</sub>H<sub>30</sub>N<sub>2</sub>O<sub>4</sub>): Calcd.: 386.2206; Obsd.: 386.2200 (–1.6 ppm).

### Synthesis of 3-(*tert*-Butyl)-4,4′-bis(6-hydroxyhexyloxy)-azobenzene (Azo-OH6)

The synthesis of Azo-OH6 was similar to the one of Azo-OH3, as illustrated in Scheme 1. Yield = 87%; m.p. 95°C; <sup>1</sup>H NMR (400 MHz, CDCl<sub>3</sub>, δ ppm): 7.90 (d, 1H, *J* = 2.40 Hz), 7.86 (d, 2H, *J* = 8.96 Hz), 7.72 (dd, 1H, *J*<sub>1</sub> = 2.40



Scheme 1. Synthetic route of azobenzene derivatives.

Hz,  $J_2 = 8.66$  Hz), 6.98 (d, 2H,  $J = 8.96$  Hz), 6.95 (d, 1H,  $J = 8.76$ ), 4.07 (m, 2H), 4.04 (m, 2H), 3.70 (m, 2H), 3.67 (m, 2H), 1.91 (m, 2H), 1.83 (m, 2H), 1.58 (m, 12H), 1.45 (s, 9H); FT-IR (KBr,  $\text{cm}^{-1}$ ): 3346, 2935, 2858, 1600, 1501, 1469, 1394, 1320, 1256, 1139, 1078, 1016, 839; HRMS ( $\text{C}_{28}\text{H}_{42}\text{N}_2\text{O}_4$ ): Calcd.: 470.3145; Obsd.: 470.3144 (−0.2 ppm).

**Synthesis of 3-(tert-Butyl)-4,4'-bisacryloxy-azobenzene (Azo-AO).** Azo-AO, Azo-AO3, and Azo-AO6 were synthesized similarly, starting from azobenzene derivatives with different alkyl chains. The procedure for Azo-AO is described below as representative: to a solution of Azo-OH (2.70 g, 10 mmol) and 15 mL of triethylamine in 200 mL of dichloromethane, 25 mL of acryloyl chloride/dichloromethane (volume ratio 1 : 4) was added via a dropping funnel. After been stirred at room temperature for 48 h, the reaction mixture was poured into deionized water. The organic layer were separated, dried over  $\text{MgSO}_4$ , concentrated and purified by column chromatography using ethyl acetate–petroleum ether (1 : 10 v/v) as eluent to give yellow solid. Yield = 89%; m.p. 152–154°C;  $^1\text{H}$  NMR (400 MHz,  $\text{CDCl}_3$ ,  $\delta$  ppm): 8.03 (d, 1H,  $J = 2.28$  Hz), 7.97 (d, 2H,  $J = 8.80$  Hz), 7.80 (dd, 1H,  $J_1 = 8.56$  Hz,  $J_2 = 2.32$  Hz), 7.30 (d, 2H,  $J = 8.80$  Hz), 7.19 (d, 1H,  $J = 8.56$  Hz), 6.67 (dd, 1H,  $J_1 = 0.90$  Hz,  $J_2 = 17.3$  Hz), 6.65 (dd, 1H,  $J_1 = 0.96$  Hz,  $J_2 = 17.3$  Hz), 6.40 (dd, 1H,  $J_1 = 10.46$  Hz,  $J_2 = 17.42$  Hz), 6.35 (dd, 1H,  $J_1 = 10.42$  Hz,  $J_2 = 17.34$  Hz), 6.10 (dd,  $J_1 = 0.90$  Hz,  $J_2 = 10.46$  Hz), 6.06 (dd, 1H,  $J_1 = 1.00$  Hz,  $J_2 = 10.48$  Hz), 1.43 (s, 9H); FT-IR (KBr,  $\text{cm}^{-1}$ ): 3462, 2969, 1740, 1633, 1593, 1490, 1403, 1295, 1243, 1221, 1186, 1159, 1075, 1017, 983, 905, 834, 801; HRMS ( $\text{C}_{22}\text{H}_{22}\text{N}_2\text{O}_4$ ): Calcd.: 378.1580; Obsd.: 378.1581 (0.3 ppm).

**Synthesis of 3-(tert-Butyl)-4,4'-bis[3-(acryloxy)propoxy]-azobenzene (Azo-AO3).** Yield = 91%; m.p. 89°C;  $^1\text{H}$  NMR (400 MHz,  $\text{CDCl}_3$ ,  $\delta$  ppm): 7.91 (d, 1H,  $J = 2.40$  Hz), 7.87 (d, 2H,  $J = 8.92$  Hz), 7.74 (dd, 1H,  $J_1 = 2.40$  Hz,  $J_2 = 8.60$  Hz), 6.98 (m, 3H), 6.44 (dd, 1H,  $J_1 = 1.32$  Hz,  $J_2 = 17.36$  Hz), 6.43 (dd, 1H,  $J_1 = 1.32$  Hz,  $J_2 = 17.32$  Hz), 6.15 (dd, 1H,  $J_1 = 10.44$  Hz,

$J_2 = 17.36$  Hz), 6.14 (dd, 1H,  $J_1 = 10.40$  Hz,  $J_2 = 17.32$  Hz), 5.86 (dd, 1H,  $J_1 = 1.36$  Hz,  $J_2 = 10.44$  Hz), 5.85 (dd, 1H,  $J_1 = 1.36$  Hz,  $J_2 = 10.44$  Hz), 4.44 (m, 2H), 4.39 (m, 2H), 4.19 (m, 2H), 4.15 (m, 2H), 2.28 (m, 2H), 2.21 (m, 2H), 1.45 (s, 9H); FT-IR (KBr,  $\text{cm}^{-1}$ ): 3443, 2966, 1720, 1637, 1598, 1497, 1472, 1409, 1297, 1241, 1206, 1145, 1062, 983, 899, 840, 818; HRMS ( $\text{C}_{28}\text{H}_{34}\text{N}_2\text{O}_6$ ): Calcd.: 494.2417; Obsd.: 494.2403 (−2.8 ppm).

**Synthesis of 3-(tert-butyl)-4,4'-bis[6-(acryloxy)hexyloxy]-azobenzene (Azo-AO6).** Yield = 38%; m.p. 46–47°C;  $^1\text{H}$  NMR (400 MHz,  $\text{CDCl}_3$ ,  $\delta$  ppm): 7.90 (d, 1H,  $J = 2.36$  Hz), 7.86 (d, 2H,  $J = 8.92$  Hz), 7.73 (dd, 1H,  $J_1 = 2.36$  Hz,  $J_2 = 8.66$  Hz), 6.98 (d, 2H,  $J = 9.00$  Hz), 6.95 (d, 1H,  $J = 8.80$  Hz), 6.43 (m, 1H), 6.39 (m, 1H), 6.14 (dd, 1H,  $J_1 = 0.64$  Hz,  $J_2 = 17.3$  Hz), 6.11 (dd, 1H,  $J_1 = 0.64$  Hz,  $J_2 = 17.3$  Hz), 5.84 (m, 1H), 5.81 (m, 1H), 4.19 (m, 4H), 4.07 (m, 2H), 4.04 (m, 2H), 1.91 (m, 2H), 1.83 (m, 2H), 1.73 (m, 4H), 1.55 (m, 8H), 1.45 (s, 9H); FT-IR (KBr,  $\text{cm}^{-1}$ ): 3433, 2952, 2861, 1726, 1637, 1584, 1501, 1474, 1451, 1405, 1296, 1236, 1194, 1142, 1077, 1010, 901, 841, 821; HRMS ( $\text{C}_{34}\text{H}_{46}\text{N}_2\text{O}_6$ ): Calcd.: 578.3356; Obsd.: 578.3359 (0.5 ppm).

#### Preparation of Pre-polymer Resin and Azo-Polymer Films

The recipes of pre-polymer resins to prepare azo-polymers AP-I, AP-II, and AP-III are listed in Table I. A transparent liquid pre-polymer resin was prepared by mixing 1 mol % of azobenzene derivative monomer, 89 mol % of MMA, 10 mol % of DPE-6A, and initiator AIBN (1 wt % relative to monomers), which were stirred overnight. The pre-polymer resin was sandwiched between a pair of clean glass slides, one of which had been modified by (heptadecafluoro-1,1,2,2-tetradecyl)trimethoxysilane to form a smooth substrate with low surface tension.<sup>32</sup> Polymerization was carried out by heating for 30 min at 75°C. A complete and uniform azo-polymer film was obtained when the untreated glass slide was removed after polymerization. The remained polymer films of AP-I, AP-II, and AP-III attached to a glass substrate were further applied to characterize the UV–Vis absorption spectra and *trans*-to-*cis* photoisomerization properties.

**Table I.** The Reaction Condition of Azo-Polymer Films

Polymer	Azobenzene monomer	MMA	DPE-6A
AP-I	Azo-AO: 1 mol %	89 mol %	10 mol %
AP-II	Azo-AO3: 1 mol %	89 mol %	10 mol %
AP-III	Azo-AO6: 1 mol %	89 mol %	10 mol %

Note: 1 wt % of AIBN is added to serve as initiator in the polymerization.

### Photoisomerization of Azo-Polymers

The research of photoresponsive behavior of azo-polymers was assisted by the irradiation from a Q-switched Nd:YAG laser at the wavelength of 355 nm (Quanta-ray INDI-Series, Spectra physics). A laser beam with a pulse width of 8 ns and a repetition rate of 10 Hz was employed as the light source to induce the *trans*-to-*cis* photoisomerization. The diameter of the laser beam was expanded to 2 cm and the average laser power used was 2 mW, which was equal to a peak power density (PPD) of laser beam about  $8 \times 10^6$  mW cm<sup>-2</sup>. Azo-polymer films were irradiated with the laser beam for 1800 s and the UV-Vis spectra over different irradiation time intervals were monitored.

### Preparation of Photoresist and TPP of PhC

TPP was carried out using the photoresist of the composition shown in Table IV, in which 1 wt % of benzil and 1 wt % of 2-benzyl-2-(dimethylamino)-4'-morpholinobutyrophenone performed as photoinitiator and photosensitizer, respectively. The mixture was stirred at room temperature overnight to form a transparent liquid before use. A mode-locked Ti : Sapphire laser system (Tsunami, Spectra-Physics) with a central wavelength of 780 nm, a pulse width of 100 fs, and a repetition rate of 82 MHz was employed to fabricate the 3D microstructures. The laser beam was tightly focused into the photoresist by an oil-immersion objective lens with a high numerical aperture (100 $\times$ , NA = 1.45, Olympus). The photoresist on the glass substrate was moved through the focus spot by a 3D piezostage (P-563.3CL, Physik Instrumente) controlled by a computer. The final structure was obtained after washing to remove the unpolymerized photoresist with acetone. The 3D microstructures were characterized by a field-emission scanning electron microscope (SEM, S-4300, Hitachi, Japan).

Transmission and reflection spectra of the PhC were measured with a Vertex 70 FT-IR system combined with a Hyperion 1000 infrared microscope equipped with a liquid-nitrogen-cooled mercury-cadmium-telluride (MCT) detector with a 36 $\times$  microscope objective (Bruker Optics GmbH, Germany). A square area was set at  $40 \times 40 \mu\text{m}^2$  for measuring by the rectangular aperture in the light path of the microscope. The PhC fabricated on a glass substrate was aligned with the surfaces perpendicular to the optical axis, which corresponds to the  $\langle 0\ 0\ 1 \rangle$  direction for the face centered tetragonal (fct) lattice symmetry. The transmission and reflection spectra were normalized to a bare glass substrate and a silver mirror, respectively. Data collection and processing were carried out using Bruker's OPUS version 6.5 software.

## RESULTS AND DISCUSSION

### Synthesis of Azobenzene Monomers and Preparation of Azo-Polymers

An important concern of this study is to design the polymerizable azobenzene derivatives with great solubility in acrylic photoresist for TPP microfabrication. The synthesis of Azo-OH via diazotization and diazo-coupling methods was referred as the first-stage reaction in the present work, as shown in Scheme 1. Introducing bulky aliphatic hydrocarbon groups and flexible alkyl chains has proved to be a very efficient method to improve the solubility of molecules in organic phase.<sup>33–35</sup> Consequently, we designed and synthesized a series of azobenzene derivatives with *tert*-butyl group in *ortho* position and two acryloxy-substituted alkyloxy groups in *para* positions, serving as monomers and crosslinkers. The molecular structures have been identified by <sup>1</sup>H NMR, MS, and FT-IR spectra.

In our previous research, it has been proved that the solubility of the new family of azobenzene monomers in photoresist significantly increases with increasing length of alkyl chains of substituent in the phenyl rings.<sup>36</sup> MMA is used as dilute monomer instead of organic solvent to dissolve other constituents. The doping concentration of Azo-AO3 and Azo-AO6 can respectively reach up to 4 mol % (about 12 wt %) and 10 mol % (about 30 wt %) in azo-polymers. The high doping concentration of azobenzene monomers in the solvent-free pre-polymer system benefit from the absence of hydrogen bonding interaction, which might have arisen the precipitation of azobenzene compounds in our previous research.<sup>29</sup>

In this study, azo-polymer films have been prepared by thermal-initiated free-radical polymerization, in which 1 mol % of different azobenzene derivatives were employed as monomers to copolymerize with 10 mol % of DPE-6A and 89 mol % of MMA without the presence of solvent or further purification processing. The multi-functional DPE-6A performed as cross-link agent to form a polymeric network, resulting that the azo-polymers were insoluble in the well-known solvent for linear PMMA.

The degree of polymerization was studied by FT-IR absorption spectra of polymer films and pre-polymer resins. As illustrated in Figure 1, the spectra of polymer films and pre-polymer resins for AP-I have been normalized to the carbonyl absorption band at 1730 cm<sup>-1</sup>, which is used as an internal standard to determine the degree of conversion of polymerizable C=C double bond in vinyl groups. The intensity of the peak at 1636 cm<sup>-1</sup> (C=C stretching of the vinyl group) has reduced by 48.6% after the polymerization, indicating the amount of C=C in vinyl groups which are opening and formation of polymeric chains. Similar situations have been observed in the spectra of AP-II and AP-III, in which the C=C stretching absorption bands of the vinyl group reduced by 47.2 and 44.4%, respectively. Meanwhile, the variations of the peak at 808 cm<sup>-1</sup> are similar, which attributed to the C-H deformation mode of the vinyl group. According to the degree of functionality and ratio of constituents in the pre-polymer resin, it could be easily predict that nearly 40% of polymerizable vinyl groups originated from DPE-6A. As there was no purification after the polymerization, the

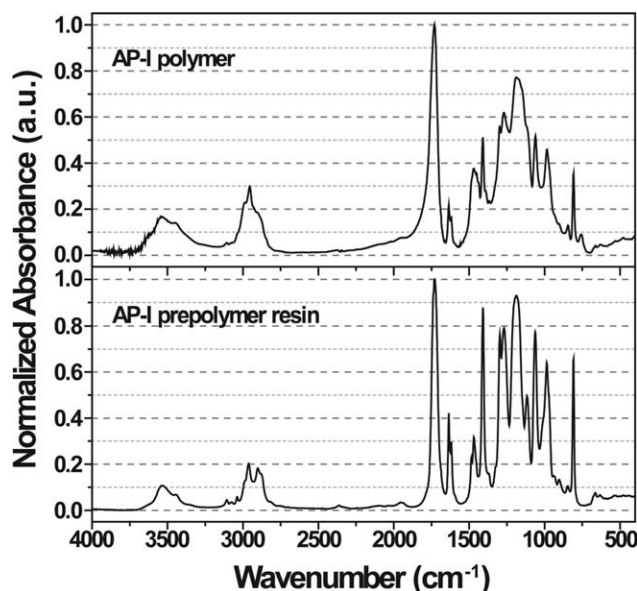


**Figure 1.** FT-IR absorption spectra of pre-polymer resin and polymer for AP-I.

FT-IR spectral analysis seems to suggest that DPE-6A was the source of most of the residual vinyl groups based on the assumption that all vinyl groups have the same reactivity. Consequently, all of the azobenzene monomers could be considered to be introduced to the polymeric chains.

An autoacceleration stage caused by the gel-effect plays a key role in the rapid formation of polymeric network. Due to the absence of solvent, parts of vinyl groups have been embedded in the highly viscous mixture and failed to participate the polymerization,<sup>37</sup> which was expressed by the residual absorptions of C=C stretching mode and C-H deformation mode of the vinyl groups in the FT-IR spectra of azo-polymer films. As a multi-branched oligomer, DPE-6A, which is usually used as a crosslink agent in UV-curing materials, retains the perfect performance in this thermal-polymerization system. Under the influence of this multi-functional reagent, autoacceleration was significantly enhanced with the increasing of crosslink density of polymeric network. Therefore, the thermal-initiated polymerization could be rapidly accomplished in less than 30 min.

The thermal stability is an important standard for the evaluation of optical materials. In this study, the thermal properties of the azo-polymers have been examined by TGA. The temperature at a 5% weight loss was recorded to regard as the initial decomposition temperature (IDT). In Figure 2, azo-polymers possess high IDT of nearly 400°C, which profit from the crosslinked polymeric network. The superior thermal stability is of great significance for applications in device manufacturing which currently concerns high temperature process, for instance, etching technology in semiconductor fabrication.<sup>38</sup>

#### Trans-to-Cis Photoisomerization

Absorption spectra of AP-I, AP-II, and AP-III films at a dark state are presented in Figure 3(a). The spectra are similar to the ones for CHCl<sub>3</sub> solutions of Azo-AO, Azo-AO3, and Azo-AO6 with the concentration of  $5 \times 10^{-5}$  mol dm<sup>-3</sup>. For each

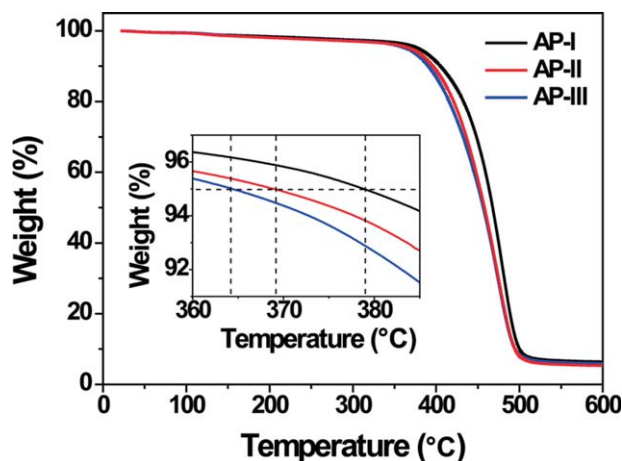


**Figure 2.** TGA curves of AP-I, AP-II, and AP-III polymers. Inset is the drawing of partial enlargement for the IDT. [Color figure can be viewed in the online issue, which is available at [wileyonlinelibrary.com](http://wileyonlinelibrary.com).]

spectrum there exists an intense absorption peak in the UV region and a weak one in the visible region, corresponding to the  $\pi-\pi^*$  and  $n-\pi^*$  electronic transition for the *trans* and *cis* isomers, respectively. The peak top wavelengths of the  $\pi-\pi^*$  electronic transition ( $\lambda_{\max}$ ) of AP-I, AP-II, and AP-III films are located at 336, 363, and 364 nm, respectively.

The kinetics of *trans*-to-*cis* photoisomerization of the prepared azo-polymer films by thermal-initiated free-radical polymerization have been studied by irradiation with 355 nm laser and monitoring the changes in the absorbance of  $\lambda_{\max}$  of the *trans* isomers. Figure 3(b,c) indicates the UV-Vis absorption spectral behavior of AP-I and AP-III films in different periods of irradiation time. As shown in the figures, when the films are irradiated by the Nd : YAG laser at 355 nm, azobenzene moieties within the azo-polymers undergo *trans*-to-*cis* photoisomerization, which is indicated by the decline of the strong *trans* and increase of the weak *cis* absorption bands. When the absorbance curves do not show significant change, the equilibrium of photostationary composition has been established. The spectra of AP-II with different irradiation time are similar with the situation of AP-III.

The relative absorbance  $A(t)$  is defined as eq. (1):

$$A(t) = \frac{\text{Abs}(\text{trans}, t)}{\text{Abs}(\text{trans}, t_0)} \quad (1)$$

where  $\text{Abs}(\text{trans}, t_0)$  and  $\text{Abs}(\text{trans}, t)$  are absorbance at  $\lambda_{\max}$  before irradiation and after the different irradiation time, respectively. In Figure 3(d), by measuring  $A(t)$  of different irradiation time ( $t$ ), the *trans*-to-*cis* photoisomerization kinetics can be best fit by a double exponential decay function [eq. (2)]:

$$A(t) = A_0 + A_1 \exp(-k_1 t) + A_2 \exp(-k_2 t) \quad (2)$$

Parameters obtained from the fitting result are summarized in Table II. The fitting function indicates that the photoisomerization of *trans* isomers consists of two processes: a faster one and a slower one. Rate constants  $k_1$  and  $k_2$  are applicable to evaluate kinetics of these two processes.

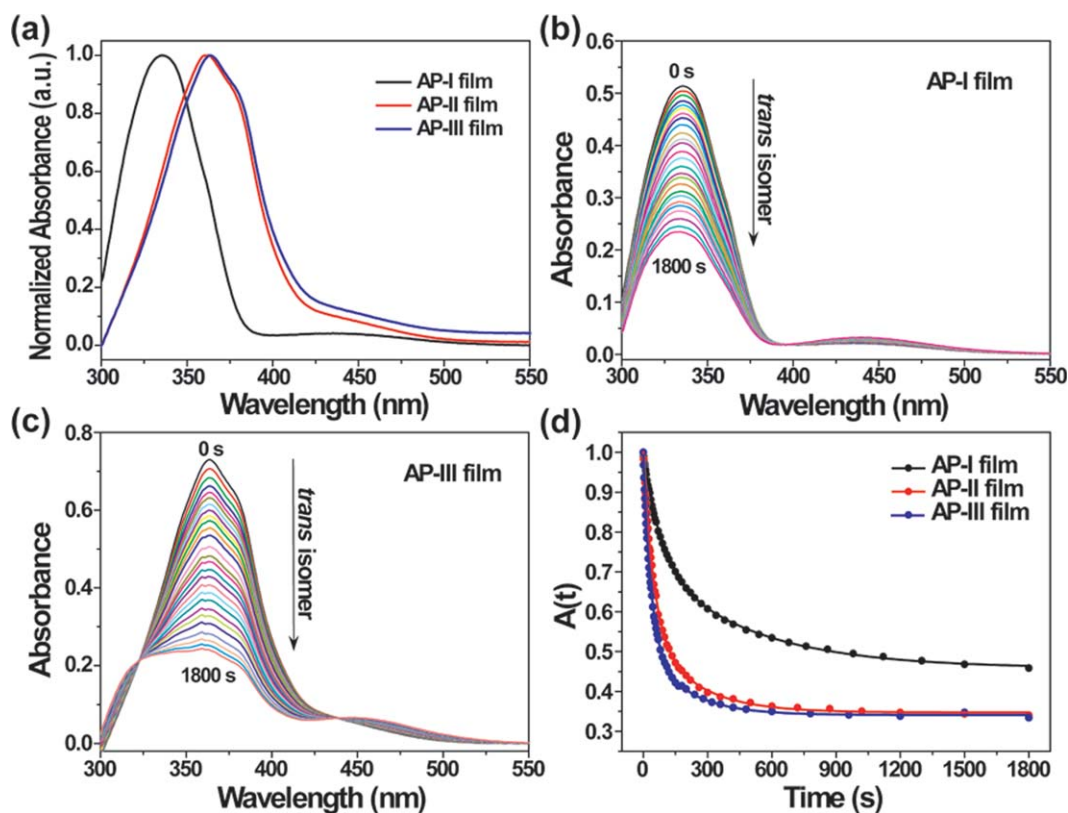


**Figure 3.** UV-Vis absorption spectra of (a) AP-I, AP-II, and AP-III films before laser irradiation, (b) AP-I and (c) AP-III films with different irradiation time. The PPD of laser was  $8.0 \times 10^6 \text{ mW cm}^{-2}$ . (d) Fitting curves of  $A(t)$ - $t$  for AP-I, AP-II, and AP-III films during the laser irradiation. [Color figure can be viewed in the online issue, which is available at [wileyonlinelibrary.com](http://www.wileyonlinelibrary.com).]

The non-first-order dynamics of photoisomerization is commonly observed in polymer systems.<sup>539–42</sup> It has been widely accepted that the photoisomerization process in bulky polymers are significantly affected by local molecular structures and free volumes of the polymeric matrix.<sup>42–46</sup> Naito and co-workers<sup>39</sup> indicated that a critical free volume that range from 0.12 to  $0.25 \text{ nm}^3$  is required to allow the isomerization of azobenzene group. In this study, the gelation stage during polymerization provides a highly crosslinked polymeric network with heterogeneous distribution of free volumes, which may play a role of effecting the motions of azobenzene chromophores.

Many studies have suggested that the dynamics of photoisomerization in polymer matrix is mainly controlled by the distribution of local free volumes around the azobenzene moieties.<sup>41,47,48</sup> In the regions where the local free volume is larger than the critical size, the photoisomerization of azobenzene groups follows a fast process, which is represented by the large rate constant  $k_1$ . Meanwhile, a part of azobenzene groups are “frozen” by the surrounding polymeric chains, where the local free volume is smaller than the critical size. This slower photoisomerization process is expressed by a smaller rate constant  $k_2$ .  $A_1$  and  $A_2$  are proportional to the numbers of azobenzene groups which following the fast and slow modes in the photoisomerization process, respectively.  $A_0$  corresponds to the fraction of residual *trans* isomers in the photostationary state on account of a lack of local free volumes and/or matrix mobility. Briefly, the heterogeneous distribution of local free volumes leads to the double exponential

dynamics of *trans*-to-*cis* photoisomerization for the azo-polymers presented in this study.

Half-life, the period of time it takes for the absorbance of *trans* form undergoing decay to decrease by half, can be calculated from eqs. (1) and (2). According to the fitting results, the ratio  $A_1/A_2$  considerably increases while half-life is shorten with enhancing length of alkyl chain in the substituent of azobenzene group, as listed in Table III. Besides,  $A_0$  also reveals to be influenced by different azobenzene species. The conversion efficiency (CE) of *trans*-to-*cis* photoisomerization at different irradiation time is estimated from eq. (3):

$$CE = \frac{A(t_0) - A(t_\infty)}{A(t_0)} \times 100\% = (1 - A_0) \times 100\% \quad (3)$$

From the fraction of residual *trans* isomers in the photostationary state ( $A_0$  in Table II), CE of *trans*-to-*cis* isomers can be estimated to be 54, 65, and 66% for AP-I, AP-II, and AP-III, respectively (Table III). It is noted that higher CE is brought about with longer alkyl chains in substitutes. The result implies that more *trans* azobenzene groups preferred to isomerize via a fast mode, as the substituent with longer alkyl chains provides larger local free volumes, which leads to faster rate and higher efficiency of photoisomerization.

An irradiation-heating cycling experiment was carried out to determine the photo-thermal stability of the azo-polymers. As described above, laser irradiation causes a progressive *trans*-to-

**Table II.** Fitting Results of the *Trans*-to-*Cis* Photoisomerization Dynamics

Polymer	$A_1$	$A_2$	$A_0$	$k_1$ ( $s^{-1}$ )	$k_2$ ( $s^{-1}$ )	$\chi^2$	$R^2$
AP-I	$0.26489 \pm 0.00766$	$0.27185 \pm 0.00652$	$0.45830 \pm 0.00235$	$0.01226 \pm 3.67032 \times 10^{-4}$	$0.00212 \pm 9.18969 \times 10^{-5}$	$5.7617 \times 10^{-6}$	0.99981
AP-II	$0.43283 \pm 0.01651$	$0.21951 \pm 0.01627$	$0.34736 \pm 0.00202$	$0.02175 \pm 7.87122 \times 10^{-4}$	$0.00463 \pm 3.73815 \times 10^{-4}$	$1.76258 \times 10^{-5}$	0.99962
AP-III	$0.46965 \pm 0.00935$	$0.18207 \pm 0.034104$	$0.34104 \pm 0.00146$	$0.02893 \pm 6.36422 \times 10^{-4}$	$0.00542 \pm 3.29761 \times 10^{-4}$	$9.97525 \times 10^{-6}$	0.99976

**Table III.** Kinetic Parameters Calculated from Eqs. (2) and (3)

Polymer	$A_1/A_2$	Half-life (s)	CE (%)
AP-I	0.97	885	54
AP-II	1.97	124	65
AP-III	2.58	83	66

*cis* photoisomerization with a photostationary state reached, meanwhile, heating to 85°C for 1 h allowed the *cis* form azobenzene chromophores to recover the initial absorption completely. The photo-thermal cycle were repeated ten times to investigate the reaction reversibility. The maximum UV-Vis absorbance at  $\lambda_{max}$  was recorded after each irradiation and heating procedure. In Figure 4, the changes of the absorbance caused by irradiation and heating are approximately the same in each irradiation-heating cycle with no signs of decline, which means that the *trans*-*cis*-*trans* isomerization is highly reversible. The excellent tunable “on-off” switching performance of the azo-polymer makes it possible to be applied to optical responsive devices.

### TPP Fabrication of the PhC

The azo-polymers not only can be prepared by the thermal-initiated polymerization of azobenzene-containing pre-polymer resins, but also can be applied to TPP with the presence of photoinitiator and photosensitizer. A photoresist, which contains 4 mol % of Azo-AO3, 10 mol % of DPE-6A, and 86 mol % of MMA as listed in Table IV, was prepared to explore the application of azo-polymers in TPP microfabrication. The woodpile geometry<sup>49</sup> is adopted for the TPP fabrication of PhC, which is designed to consist of forty and five periods in the <1 1 0> and <0 0 1> directions, respectively. The axes of the rods for each horizontal layer are designed to arrange with an in-plane

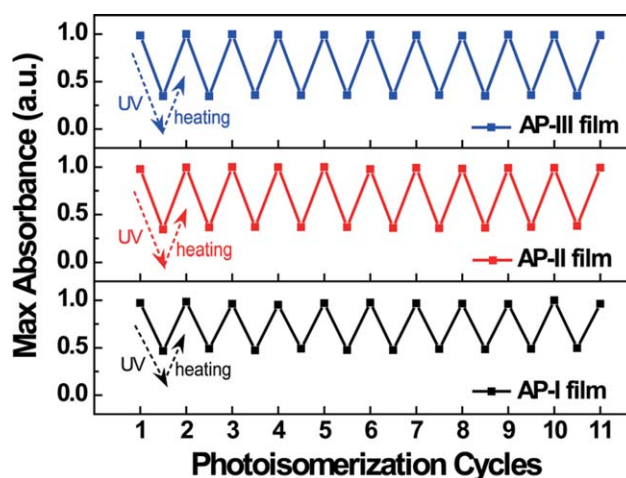


**Figure 4.** Normalized maximum absorbance of  $\pi$ - $\pi^*$  electronic transition band during the irradiation-heating cycles between the *trans* and the *cis* form azobenzene configurations for AP-I, AP-II, and AP-III films. The PPD of laser was  $8.0 \times 10^6$   $mW\ cm^{-2}$  and the irradiation time was 30 min. The heating experiment was carried out by heating the samples to 85°C for 1 h. [Color figure can be viewed in the online issue, which is available at [wileyonlinelibrary.com](http://wileyonlinelibrary.com).]

**Table IV.** The Photoresist for TPP Fabrication

Azo-AO3	DPE-6A	MMA	Photoinitiator	Photosensitizer
4 mol %	10 mol %	86 mol %	1 wt %	1 wt %

Note: The weight percents of photoinitiator and photosensitizer are relative to the total amount of Azo-AO3, DPE-6A, and MMA.

spacing of 850 nm in the  $\langle 1\ 1\ 0 \rangle$  direction. Correspondingly, the periodicity in the  $\langle 0\ 0\ 1 \rangle$  direction is 1202 nm according to the fct lattice symmetry. For the cross section of each rod, the width in the  $\langle 1\ 1\ 0 \rangle$  direction and the height in the  $\langle 0\ 0\ 1 \rangle$  direction are designed as 200 and 250 nm, respectively.

With the method of TPP, a woodpile PhC has been successfully fabricated with the photoresist in Table IV using a femtosecond laser at the wavelength of 780 nm with the average power of 4.8 mW (measured on the front of the objective lens) and the scan velocity of 120 nm ms<sup>-1</sup>. Figure 5 shows SEM images and details of the structure. For each rod, a resolution of approximately 180 nm in the width is achieved, with a periodicity of 950 nm in the  $\langle 1\ 1\ 0 \rangle$  direction.

To evaluate the fabrication quality of the 3D structure, we performed measurements of transmission and reflection spectra assisted by a FT-IR spectrometer with an infrared microscope. As displayed in Figure 6, the center wavelengths of maximum reflection and minimum transmission appear at 1334 and 1293 nm, respectively. The existence of PBG along the stacking

direction  $\langle 0\ 0\ 1 \rangle$  is signified by the existence of the strong stop gap, which is located in the 1.3  $\mu\text{m}$  telecommunication wavelength region.

The simulations of frequency spectra for the PhC with designed structural parameters were performed using the commercially available software Comsol Multiphysics. A refractive index of 1.504 for the azo-polymer determined at 1315 nm by the m-line prism coupling technique<sup>50</sup> was applied in the simulations. In Figure 6, according to the simulated results, there exist maximum reflection and minimum transmission peaks around 200–230 THz, corresponding to the wavelength region of 1300–1500 nm for the designed structure, which are in good agreement with the measured results. It is noted that there is a slight deviation in the measured result of transmission spectrum from the simulated one, which may be attributed to the inevitable defects and the deformation of the microstructure resulting from the developing process in the TPP fabrication.

As the refractive indices of azo-polymers could be regulated via the *trans-cis* photoisomerization,<sup>3,4,51</sup> we expected that the PBG

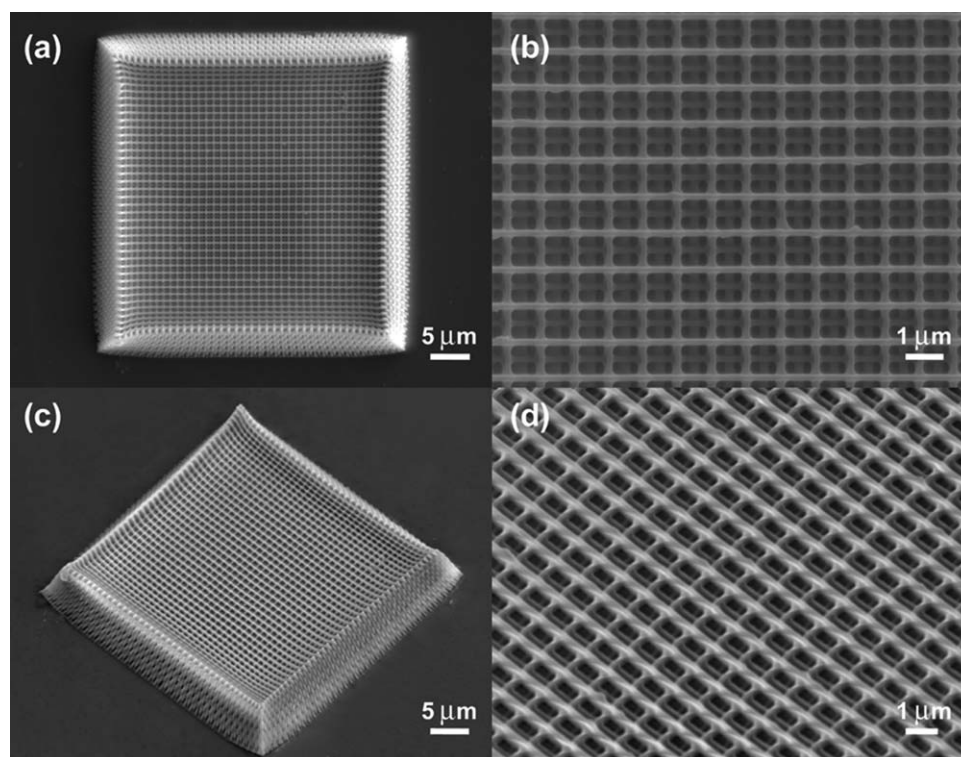


**Figure 5.** SEM images of the woodpile PhC fabricated with the photoresist in Table IV. (a) Top view of the PhC. (b) Locally magnified image of the top layer. (c) Side view of the PhC. (d) Locally magnified image of c.



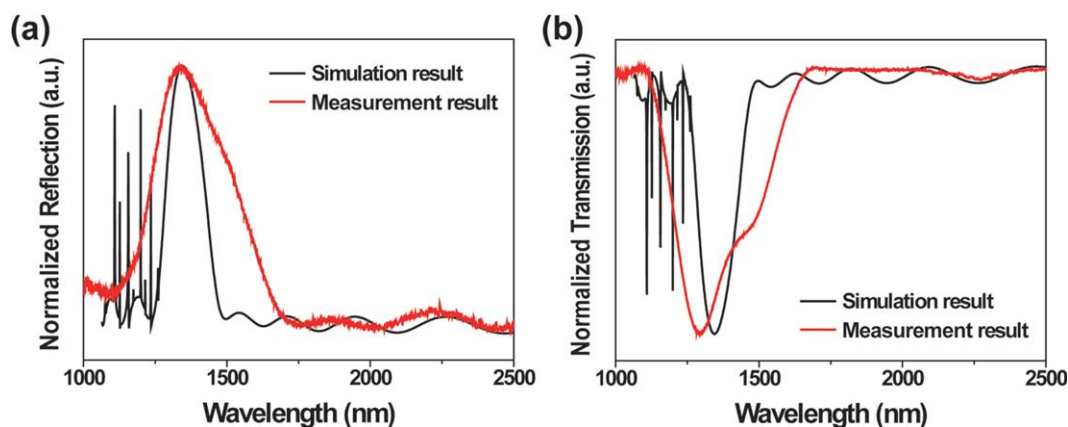


**Figure 6.** (a) Reflection and (b) transmission spectra of simulated and measured results for the woodpile PhC at  $\langle 0\ 0\ 1 \rangle$  direction. [Color figure can be viewed in the online issue, which is available at [wileyonlinelibrary.com](http://wileyonlinelibrary.com).]

of a PhC composed of azo-polymers would be tunable by the means of pumping with different light resources.<sup>28</sup> Nevertheless, for the azo-polymer containing 4 mol % of Azo-AO3, the change of the refractive index in the photoisomerization is only 0.004, which may be too small to induce the tuning of the PBG. In spite of this, the result clearly indicates that the azobenzene-containing photoresist performs very well in TPP and will hopefully be used to fabricate complicated 3D optical communication micro/nano devices. Further research on photoresponse behaviors of micro/nano structure based on azo-polymers will be investigated in our next study.

## CONCLUSION

In conclusion, we designed and synthesized a series of azo-polymers, and demonstrated their *trans*-to-*cis* photoisomerization behaviors and application in TPP microfabrication. By introducing bulky *tert*-butyl and flexible alkyl chains, azobenzene derivatives with good solubility were synthesized and employed as monomers and/or crosslinkers for the preparation of azo-polymers. The *trans*-to-*cis* photopolymerization of azo-polymers followed a double exponential dynamics, which was caused by the complicated motions of azobenzene moieties in the crosslinked polymeric matrix. The azo-polymers manifested superior photo-thermal stability and “on-off” switching effect. The photoresist containing the synthesized azobenzene derivative exhibited excellent TPP performance in the fabrication of 3D PhC with PBG in the near-infrared wavelength region. With the great chemical properties and fabrication performance, it is expected that the azo-polymers will promote progress in manufacturing of optical functional devices.

## ACKNOWLEDGMENT

The authors are grateful to the National Natural Science Foundation of China (Grant Nos. 61275171, 51003113, 61275048, 91123032), the National Basic Research Program of China (2010CB934103), International Cooperation Program of MOST (2010DFA01180), and Doctoral Candidate Innovation Research Support Program by Science and Technology Review (kjdb201001-5) for financial support.

## REFERENCES

1. Yu, Y.; Nakano, M.; Ikeda, T. *Nature* **2003**, *425*, 145.
2. Buechel, M.; Sekkat, Z.; Paul, S.; Weichart, B.; Menzel, H.; Knoll, W. *Langmuir* **1995**, *11*, 4460.
3. Natansohn, A.; Rochon, P.; Gosselin, J.; Xie, S. *Macromolecules* **1992**, *25*, 2268.
4. Natansohn, A.; Xie, S.; Rochon, P. *Macromolecules* **1992**, *25*, 5531.
5. Ho, M. S.; Natansohn, A.; Rochon, P. *Macromolecules* **1995**, *28*, 6124.
6. Kim, D.; Tripathy, S.; Li, L.; Kumar, J. *Appl. Phys. Lett.* **1995**, *66*, 1166.
7. Rochon, P.; Batalla, E.; Natansohn, A. *Appl. Phys. Lett.* **1995**, *66*, 136.
8. Huang, J.; Wu, S.; Beckemper, S.; Gillner, A.; Zhang, Q.; Wang, K. *Opt. Lett.* **2010**, *35*, 2711.
9. Nakanishi, M.; Sugihara, O.; Okamoto, N.; Hirota, K. *Appl. Opt.* **1998**, *37*, 1068.
10. Kang, J. W.; Kim, M. J.; Kim, J. P.; Yoo, S. J.; Lee, J. S.; Kim, D. Y.; Kim, J. J. *Appl. Phys. Lett.* **2003**, *82*, 3823.
11. Kawata, S.; Sun, H. B.; Tanaka, T.; Takada, K. *Nature* **2001**, *412*, 697.
12. Tan, D.; Li, Y.; Qi, F.; Yang, H.; Gong, Q.; Dong, X.; Duan, X. *Appl. Phys. Lett.* **2007**, *90*, 071106.
13. Xing, J.-F.; Dong, X.-Z.; Chen, W.-Q.; Duan, X.-M.; Takeyasu, N.; Tanaka, T.; Kawata, S. *Appl. Phys. Lett.* **2007**, *90*, 131106.
14. Dong, X.-Z.; Zhao, Z.-S.; Duan, X.-M. *Appl. Phys. Lett.* **2008**, *92*, 091113.
15. Farsari, M.; Ovsianikov, A.; Vamvakaki, M.; Sakellari, I.; Gray, D.; Chichkov, B.; Fotakis, C. *Appl. Phys. Part A: Mater. Sci. Process.* **2008**, *93*, 11.
16. Sun, Z. B.; Dong, X. Z.; Chen, W. Q.; Nakanishi, S.; Duan, X. M.; Kawata, S. *Adv. Mater.* **2008**, *20*, 914.
17. Xia, H.; Wang, J.; Tian, Y.; Chen, Q. D.; Du, X. B.; Zhang, Y. L.; He, Y.; Sun, H. B. *Adv. Mater.* **2010**, *22*, 3204.
18. Kaneko, K.; Sun, H.-B.; Duan, X.-M.; Kawata, S. *Appl. Phys. Lett.* **2003**, *83*, 1426.

19. Cao, Y. Y.; Takeyasu, N.; Tanaka, T.; Duan, X. M.; Kawata, S. *Small* **2009**, *5*, 1144.
20. Wang, W.-K.; Sun, Z.-B.; Zheng, M.-L.; Dong, X.-Z.; Zhao, Z.-S.; Duan, X.-M. *J. Phys. Chem. C* **2011**, *115*, 11275.
21. Sun, H. B.; Matsuo, S.; Misawa, H. *Appl. Phys. Lett.* **1999**, *74*, 786.
22. Dong, X.-Z.; Ya, Q.; Sheng, X.-Z.; Li, Z.-Y.; Zhao, Z.-S.; Duan, X.-M. *Appl. Phys. Lett.* **2008**, *92*, 231103.
23. Joshi, M. P.; Pudavar, H. E.; Swiatkiewicz, J.; Prasad, P.; Reianhardt, B. *Appl. Phys. Lett.* **1999**, *74*, 170.
24. Kowalevicz, A. M.; Sharma, V.; Ippen, E. P.; Fujimoto, J. G.; Minoshima, K. *Opt. Lett.* **2005**, *30*, 1060.
25. Nishiyama, H.; Nishii, J.; Mizoshiri, M.; Hirata, Y. *Appl. Surf. Sci.* **2009**, *255*, 9750.
26. Guo, R.; Xiao, S.; Zhai, X.; Li, J.; Xia, A.; Huang, W. *Opt. Express* **2006**, *14*, 810.
27. Li, C.-F.; Dong, X.-Z.; Jin, F.; Jin, W.; Chen, W.-Q.; Zhao, Z.-S.; Duan, X.-M. *Appl. Phys. Part A: Mater. Sci. Process.* **2007**, *89*, 145.
28. Ya, Q.; Chen, W. Q.; Dong, X. Z.; Rodgers, T.; Nakanishi, S.; Shoji, S.; Duan, X. M.; Kawata, S. *Appl. Phys. Part A: Mater. Sci. Process.* **2008**, *93*, 393.
29. Ya, Q.; Dong, X. Z.; Chen, W. Q.; Duan, X. M. *Dyes. Pigments* **2008**, *79*, 159.
30. Angeloni, A. S.; Caretti, D.; Carlini, C.; Chiellini, E.; Galli, G.; Altomare, A.; Solaro, R.; Laus, M. *Liq. Cryst.* **1989**, *4*, 513.
31. Kang, H.; Lee, B.; Yoon, J.; Yoon, M. *J. Colloid. Interf. Sci.* **2000**, *231*, 255.
32. Li, Z.; Meng, X.; Tang, F. *J. Nanosci. Nanotechnol.* **2011**, *11*, 10158.
33. Ayala, D.; Lozano, A. E.; De Abajo, J.; De La Campa, J. G. *J. Polym. Sci. Part A: Pol. Chem.* **1999**, *37*, 805.
34. Kitamura, C.; Tanaka, S.; Yamashita, Y. *Chem. Mater.* **1996**, *8*, 570.
35. Elsenbaumer, R.; Jen, K.; Oboodi, R. *Synth. Met.* **1986**, *15*, 169.
36. Wang, H.; Chen, W. Q.; Jin, F.; Dong, X. Z.; Zhao, Z. S.; Duan, X. M. Photoisomerization of Azobenzene Moiety in Crosslinking Polymer Materials; In Proceedings of SPIE 8474, Optical Processes in Organic Materials and Nanostructures, San Diego, California, USA, August 12, **2012**; Jakubiak, R.; Eich, M. and Nunzi, J. M.; Eds.; SPIE: Bellingham, **2012**.
37. Flory, P. J. Principles of Polymer Chemistry; Cornell University Press: New York, **1953**; Chapter 4, pp 124–129.
38. Yu, X.; Luo, Y.; Deng, Y.; Yan, Q.; Zou, G.; Zhang, Q. *Eur. Polym. J.* **2008**, *44*, 881.
39. Naito, T.; Horie, K.; Mita, I. *Macromolecules* **1991**, *24*, 2907.
40. Dante, S.; Advincula, R.; Frank, C. W.; Stroeve, P. *Langmuir* **1999**, *15*, 193.
41. Tateishi, Y.; Tanaka, K.; Nagamura, T. *J. Phys. Chem. B* **2007**, *111*, 7761.
42. Verborgt, J.; Smets, G. *J. Polym. Sci.* **1974**, *12*, 2511.
43. Xie, S.; Natansohn, A.; Rochon, P. *Chem. Mater.* **1993**, *5*, 403.
44. Eisenbach, C. D. *Berich. Bunsen. Gesell.* **1980**, *84*, 680.
45. Kumar, G. S.; Savariar, C.; Saffran, M.; Neckers, D. *Macromolecules* **1985**, *18*, 1525.
46. Kumar, G. S.; Neckers, D. C. *Chem. Rev.* **1989**, *89*, 1915.
47. Yu, W. C.; Sung, C. S. P. *Macromolecules* **1988**, *21*, 365.
48. Naito, T.; Kunishige, M.; Yamashita, T.; Horie, K.; Mita, I. *React. Polym.* **1991**, *15*, 185.
49. Lin, S.; Fleming, J.; Hetherington, D.; Smith, B.; Biswas, R.; Ho, K.; Sigalas, M.; Zubrzycki, W.; Kurtz, S.; Bur, J. *Nature* **1998**, *394*, 251.
50. Monneret, S.; Huguet-Chantôme, P.; Flory, F. *J. Opt. Part A: Pure Appl. Opt.* **2000**, *2*, 188.
51. Murase, S.; Horie, K. *Macromolecules* **1999**, *32*, 1103.